

## Effects of oxygen and illumination on the *in situ* conductivity of C<sub>60</sub> thin films

A. Hamed, Y. Y. Sun, Y. K. Tao, R. L. Meng, and P. H. Hor

*Texas Center for Superconductivity at the University of Houston, Houston, Texas 77204-5932*

(Received 19 August 1992; revised manuscript received 18 January 1993)

We report *in situ* measurements of dc conductivity versus temperature in polycrystalline films of C<sub>60</sub>. Films sublimed using C<sub>60</sub> powders from different batches synthesized according to standard techniques were used in conductivity versus temperature measurements in the range 20–180 °C. The films showed clear semiconductor behavior. Activation energies  $E_a$  and room-temperature dark conductivities  $\sigma$  were in the range 0.54–0.58 eV and  $10^{-6}$ – $10^{-7}$  ( $\Omega$  cm)<sup>-1</sup>, respectively. Exposing the films to pure O<sub>2</sub> or air at 21 °C leads to a fast decrease in dark conductivity and photoconductivity by orders of magnitude, indicating that oxygen quickly permeates the whole depth of the films. This indicates that at room temperature O<sub>2</sub> quickly diffuses into the bulk of C<sub>60</sub> and changes the electronic properties of the material. Most of the effect of oxygen on the conductivity can be reversed in minutes by increasing the temperature of the films to 160–180 °C in vacuum, but the final state has slightly larger resistivity and activation energy. Exposure of C<sub>60</sub> films at 21 °C to Ar, N<sub>2</sub>, and He gases had no effect on  $\sigma$ . Illumination of the films in the presence of O<sub>2</sub> causes larger and faster irreversible changes in  $\sigma$  and  $E_a$ . In particular, exposing a 165-nm-thick film having  $\sigma(21\text{ °C}) \sim 10^{-6}$  ( $\Omega$  cm)<sup>-1</sup> and  $E_a = 0.54$  eV to a white-light intensity of 60 mW/cm<sup>2</sup> in 1 atm O<sub>2</sub> at 21 °C for 1 h yields a state, after annealing, exhibiting  $\sigma(21\text{ °C}) \sim 10^{-14}$  ( $\Omega$  cm)<sup>-1</sup> and  $E_a = 0.95$  eV. The effect of pure O<sub>2</sub> on the conductivity of solid C<sub>60</sub> can be explained in terms of a disorder potential that leads to localization of the electronic states at the edges of the highest-occupied-molecular-orbital- and lowest-unoccupied-molecular-orbital-derived bands. In addition, oxygen may act as an efficient trap for electrons in the conduction band of C<sub>60</sub>. Illumination of the samples in the presence of oxygen promotes C-O reactions that irreversibly damage the C<sub>60</sub> molecules, producing carbon dangling bonds and other defects that possibly generate gap-defect states in the semiconductor. The results of the present study also suggest that measured optical properties of C<sub>60</sub> in the low-photon-energy range may be affected by oxygen contamination and strong light.

### I. INTRODUCTION

After the 1985 discovery of the high stability of the C<sub>60</sub> molecule,<sup>1</sup> there followed, five years later, a simple method for producing macroscopic quantities of C<sub>60</sub> powder<sup>2</sup> that led to an intense and ongoing research effort on this form of carbon. The existence of superconducting transition temperatures in the range 18–32 K in alkali-doped C<sub>60</sub> (Refs. 3–6) has stimulated considerable work on the transport properties of the normal and superconducting states of these compounds, but few experimental studies have focused on the electronic transport properties of pure C<sub>60</sub>.<sup>7–9</sup>

In its pure solid form, C<sub>60</sub> is a molecular semiconductor,<sup>5,10,11</sup> with the molecular unit consisting of 60 carbon atoms arranged in a nearly spherical structure<sup>1,2</sup> having a radius of 0.35 nm,<sup>12,13</sup> and with the C<sub>60</sub> molecules sitting, at room temperature, on the sites of a fcc lattice with lattice parameter  $a = 1.417$  nm.<sup>14</sup> The interesting chemical properties of the C<sub>60</sub> molecule,<sup>15</sup> the feasibility of introducing atoms inside the C<sub>60</sub> cage<sup>16–19</sup> and of substituting a few carbon atoms on the spherical shell by a different species,<sup>16</sup> open up a wealth of possibilities for the synthesis of new compounds having highly unusual properties. It has already been suggested<sup>20</sup> that the large intermolecular distance ( $\sim 1$  nm) between the closed-packed C<sub>60</sub> molecules may lead to nanometer-scale-engineered thin-film structures. A necessary step, however, is to gain

a better understanding of the intrinsic properties of C<sub>60</sub> and to study how they are affected when the material is exposed to various experimental factors.

Oxygen contamination of C<sub>60</sub> can produce misleading results. For example, the Raman line at 1467 cm<sup>-1</sup>, a mode previously attributed to pure C<sub>60</sub>, appears only after oxygen exposure.<sup>21,22</sup> The effects of oxygen on C<sub>60</sub> can be severe. For powder samples in pure oxygen at moderate temperatures of 200 °C, the fcc C<sub>60</sub> transforms into amorphous carbon-oxygen compounds, and the icosahedral C<sub>60</sub> molecular structure is destroyed.<sup>23,24</sup> Photoemission studies of solid O<sub>2</sub> in contact with thin films of C<sub>60</sub> held at 20 K show that, upon exposure to low-energy ( $\sim 0.5$ – $5$ -eV) or high-energy ( $\sim 2$ – $1200$ -eV) photons, C<sub>60</sub> partially converts to CO, CO<sub>2</sub>, carbonyl-like structures, and amorphous carbon.<sup>25</sup> The degradation of C<sub>60</sub> powder stored at room temperature without exclusion of light or oxygen has also been noticed,<sup>26</sup> and prolonged (10–16-h) ultraviolet irradiation of room-temperature solutions of C<sub>60</sub> in hexane leads to substantial or complete fragmentation of the C<sub>60</sub> cage.<sup>26</sup>

The earliest report on conductivity in pristine C<sub>60</sub> films was made in connection with the first studies of doped C<sub>60</sub> films, where an upper limit of  $10^{-5}$  ( $\Omega$  cm)<sup>-1</sup> was given for the conductivity near room temperature.<sup>27</sup> Semiconducting behavior in the temperature-dependent conductivity has been observed<sup>28</sup> in lightly doped K<sub>x</sub>C<sub>60</sub> as well as in C<sub>60/70</sub> films.<sup>7–9</sup> In the present study, we

prepare thin films of  $C_{60}$  under high vacuum by sublimation of  $C_{60}$  powder whose exposure to air and light has been minimized, and we measure *in situ* photoconductivity and temperature dependence and activation energy of the dark conductivity. We determine how these quantities are affected by controlled exposure of the films to light and/or oxygen, and study the reversibility of the observed effects. In addition to  $O_2$ , we also expose  $C_{60}$  films to  $N_2$ , Ar, and He gases. Given the exponential dependence of conductivity on the position of the Fermi level in a semiconductor, conductivity measurements can provide an extremely sensitive way of monitoring changes in the density of electronic states in the gap or near the band edges of  $C_{60}$  caused by light, oxygen, and other agents.

## II. EXPERIMENTAL DETAILS

$C_{60}$  powder was synthesized according to standard techniques.<sup>29,30</sup> In brief, carbon soot containing  $C_{60}$  and other forms of carbon was produced by arc discharge between two closely spaced high-purity graphite rods in a 100-Torr He atmosphere.  $C_{60}$  was then separated from the soot using toluene and purified by liquid chromatography involving a neutral alumina column in hexanes. The resulting  $C_{60}$  powder was then washed in ethyl ether, dried at 120°C in vacuum for 12 h, followed by another 12 h at 300–350°C in  $N_2$  flow, and finally stored protected from light in a desiccator. A small amount of the  $C_{60}$  powder was later placed in a quartz crucible in an evaporation-measurement system having a base pressure of  $1.5 \times 10^{-7}$  Torr. The powder was degassed *in situ* at 250–300°C for several hours and then sublimed at temperatures 450–500°C. A shutter protecting the substrates was open only after a constant and stable evaporation rate of 0.03 nm/s, as detected by a quartz-crystal monitor, had been reached. Final film thicknesses were later verified with a profilometer. Substrate temperature was kept at 180°C during film growth, based on evidence that films grown at about 200°C have better morphology than those grown at room temperature.<sup>31</sup>

For the *in situ* two-probe coplanar conductivity measurements, several equally spaced Ag or Ni electrodes, having a length of 0.3 cm and a gap of 0.15 cm, were preevaporated on 1.2-cm-long carefully cleaned sapphire substrates. Pt wires were attached to one edge of the electrodes with silver paste. The various electrodes were used to verify the uniformity of the films. Ag electrodes exhibited ohmic behavior up to the maximum  $10^3$ -V/cm applied field. *In situ* illumination of the films was carried out through a high-vacuum infrared-absorbing window using white light from a tungsten-halogen projector lamp. In measurements of the temperature dependence of the conductivity, we used heating and cooling rates of 2°C/min.

X-ray analysis of the films indicated polycrystallinity and fcc structure. Raman spectra showed no  $C_{70}$  to a resolution of 2%. Scanning-electron-microscope (SEM) images with a resolution of 100 nm showed uniform sur-

face morphology, and TEM images revealed crystal grain sizes between 20 and 200 nm.

## III. RESULTS

Figure 1 shows the conductance  $G$  as a function of film thickness  $d$  for a  $C_{60}$  film (film 1). Both  $G$  and  $d$  are monitored *in situ* during film growth. After an exponential climb below 40 nm, the conductance continues to grow rapidly between 40 and 70 nm at a decreasing rate. Above 70 nm, there is a linear regime that extrapolates to the origin in a linear plot of  $G$  versus  $d$ . This later observation indicates that we are able to measure bulk conductivity in our  $C_{60}$  thin film without the complication of highly conductive surface carrier accumulation or depletion layers. The onset of the linear regime and the details of the nonlinear region at small  $d$  might be expected to change with growth rate and with the substrate temperature during film growth, which we shall call the deposition temperature. The deposition of film 1 was continued to a final thickness of 165 nm, and kept at the deposition temperature of 180°C for several hours to test for possible relaxation, but no change in  $G$  was observed. Conductivity values  $\sigma$  can be obtained from the conductance values  $G$  using  $\sigma = 0.50 \times d^{-1} \times G$ , where the factor 0.5 is given by the electrode geometry.

In Fig. 2(a), we plot  $\sigma$  as a function of inverse temperature between 15 and 180°C, measured on cooling (circles) and heating (triangles). A straight line is obtained in most of the temperature range, clearly indicating the semiconductor character of  $C_{60}$ . Such a line is described by an equation of the form  $\sigma = \sigma_0 \exp(-E_a/kT)$ , where  $\sigma_0$  is the conductivity prefactor,  $k$  the Boltzmann constant,  $T$  the absolute temperature, and  $E_a$ , the activation

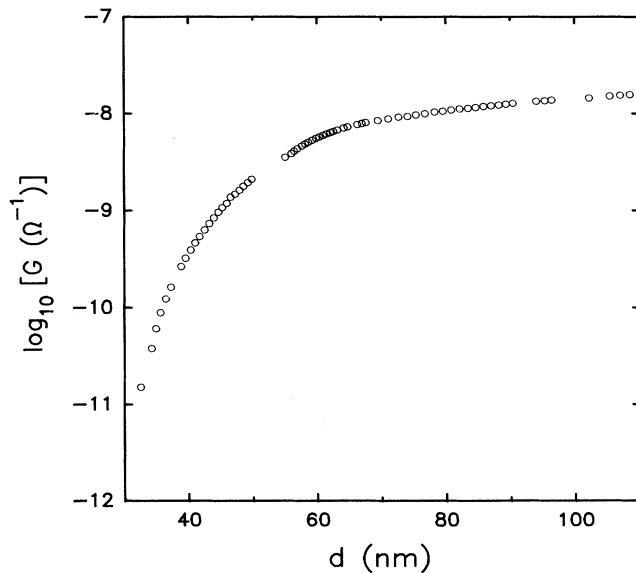


FIG. 1. The conductance  $G$  as a function of the thickness  $d$  for a thin film of  $C_{60}$  at 180°C. Both quantities are monitored *in situ* during growth.

energy, is a measure of the energy distance between the Fermi level and the band edge in the semiconductor. From the line drawn through the data points in Fig. 2(a), the values  $E_a = 0.54$  eV and  $\sigma_0 = 1.5 \times 10^3$  ( $\Omega \text{ cm}$ ) $^{-1}$  are

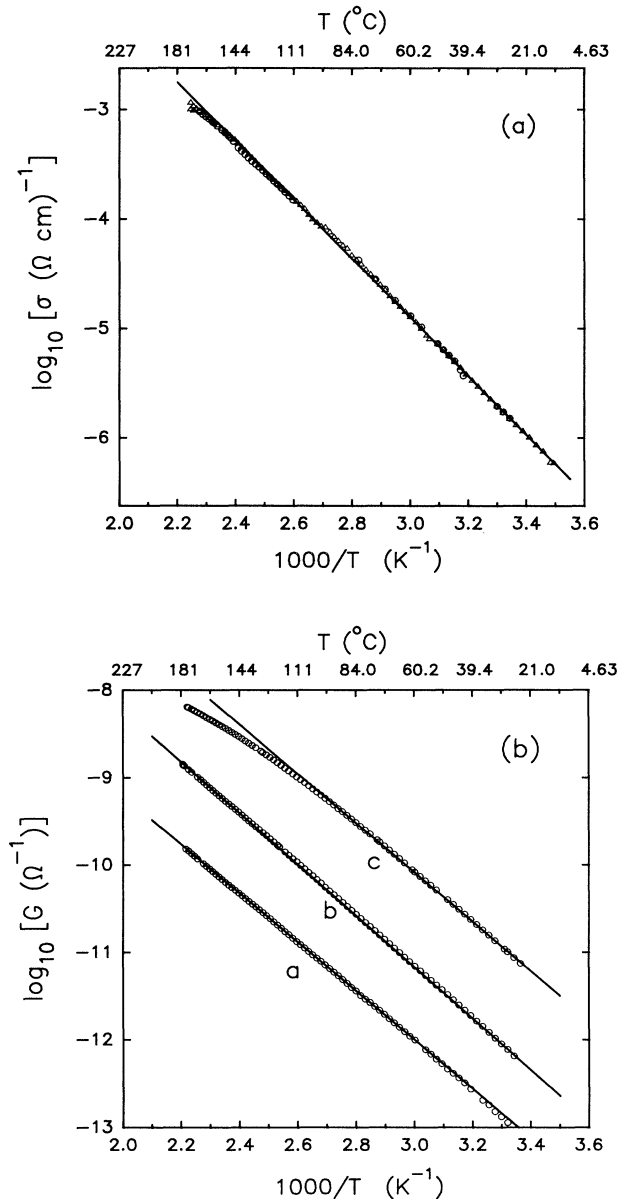


FIG. 2. (a) The temperature dependence of the *in situ* conductivity  $\sigma$  for a 165-nm-thick  $\text{C}_{60}$  film (film 1), measured on cooling (circles) and heating (triangles). The conductivity at 21 °C is  $\sigma(21^\circ\text{C}) = 8.3 \times 10^{-7}$  ( $\Omega \text{ cm}$ ) $^{-1}$ . From the line drawn through the data points, an activation energy  $E_a = 0.54$  eV is obtained. (b) The temperature dependence of the conductance  $G$  of film 2 obtained at different stages of the growth process, corresponding to film thicknesses  $d = 58$  nm (curve *a*), 85 nm (curve *b*), and 350 nm (curve *c*), exhibiting  $\sigma(21^\circ\text{C}) = 6.5 \times 10^{-9}$ ,  $2.6 \times 10^{-8}$ , and  $9.8 \times 10^{-8}$  ( $\Omega \text{ cm}$ ) $^{-1}$ , respectively. From the lines drawn, one obtains activation energies  $E_a = 0.55$ , 0.58, and 0.56 eV for curves *a*, *b*, and *c*, respectively.

derived. The dark conductivity at 21 °C is  $\sigma(21^\circ\text{C}) = 8.3 \times 10^{-7}$  ( $\Omega \text{ cm}$ ) $^{-1}$ . The data points in Fig. 2(a) exhibit a slight downwards curvature between 160 and 180 °C.

Figure 2(b) gives the temperature dependence of the conductance  $G$  (rather than  $\sigma$ ) for a second film (film 2) at three stages of the growth process. As before, conductivity values can be obtained from  $\sigma = 0.50 \times d^{-1} \times G$ . Deposition was interrupted at  $d = 58$ , 85, and 350 nm and curves *a*, *b*, and *c* were obtained. First, we notice that curve *a* is a straight line in the whole temperature range 20–180 °C, curve *b* has a barely noticeable downwards curvature above 130 °C, and curve *c* exhibits a clear curvature above 110 °C. All curves were reproducible upon heating and cooling. Figures 2(a) and 2(b) suggest that a downwards curvature in the  $G$  versus  $1/T$  plot is observable at large enough values of  $d$ , becoming more pronounced with increasing  $d$ . From the lines in Fig. 2(b), one obtains the values  $E_a = 0.55$  eV,  $\sigma_0 = 1.8 \times 10^1$  ( $\Omega \text{ cm}$ ) $^{-1}$ , and  $\sigma(21^\circ\text{C}) = 6.5 \times 10^{-9}$  ( $\Omega \text{ cm}$ ) $^{-1}$  for curve *a*,  $E_a = 0.58$  eV,  $\sigma_0 = 2.0 \times 10^2$  ( $\Omega \text{ cm}$ ) $^{-1}$ , and  $\sigma(21^\circ\text{C}) = 2.6 \times 10^{-8}$  ( $\Omega \text{ cm}$ ) $^{-1}$  for curve *b*, and  $E_a = 0.56$  eV,  $\sigma_0 = 3.5 \times 10^2$  ( $\Omega \text{ cm}$ ) $^{-1}$ , and  $\sigma(21^\circ\text{C}) = 9.8 \times 10^{-8}$  ( $\Omega \text{ cm}$ ) $^{-1}$  for curve *c*. We also note that the  $G$  values scale with film thickness  $d$  for curves *b* and *c*, indicating bulk conductivity, but not for curve *a* ( $d = 58$  nm). This is consistent with the behavior of  $G$  versus  $d$  already observed for film 1 in Fig. 1.

Films 1 ( $d = 165$  nm) and 2 ( $d = 350$  nm) have similar activation energies, but film 2, being twice as thick, is a factor of 10 more resistive. The  $\text{C}_{60}$  powders used for preparing films 1 and 2 were synthesized according to the same procedure but belonged to different batches, and even though their exposure to air and light was minimized, it could not be completely eliminated. In view of the experimental results presented below, it is possible that powders with slightly different degrees of exposure to light and air will lead to films of different conductivity. In any case, what is of relevance for the results presented below is that both films 1 and 2 exhibited qualitatively and quantitatively similar effects when exposed to light and oxygen. In what follows, we present results for film 1.

Figure 3 shows the effect of light on the dark conductivity  $\sigma$  and photoconductivity  $\sigma_{\text{ph}}$  of film 1 in a vacuum of  $10^{-7}$  Torr. We approximate  $\sigma_{\text{ph}} = \sigma_{\text{il}} - \sigma \approx \sigma_{\text{il}}$ , where  $\sigma_{\text{il}}$  is the conductivity measured under illumination. The sample is illuminated at 25 °C with increasing white-light intensities from  $\sim 15$  to  $\sim 60$  mW/cm $^2$ . For an intensity  $\sim 15$  mW/cm $^2$ ,  $\sigma_{\text{ph}}$  is about six times larger than  $\sigma$ . Even for this moderate light intensity, it is possible to observe a small but sustained decrease in  $\sigma_{\text{ph}}$  with exposure time  $t_e$  on a time scale of minutes. Upon turning the light off after  $t_e = 5$  min,  $\sigma$  drops below its original (before illumination) value. These effects are more significant at larger light intensities, as seen in Fig. 3. At the light intensity 60 mW/cm $^2$ ,  $\sigma_{\text{ph}}$  is about 60 times larger than  $\sigma$ . After  $t_e = 24$  h with 60 mW/cm $^2$ , both  $\sigma_{\text{ph}}$  and  $\sigma$  decrease by a factor of 10, as shown by the two data points on the right side of the axis break in Fig. 3.

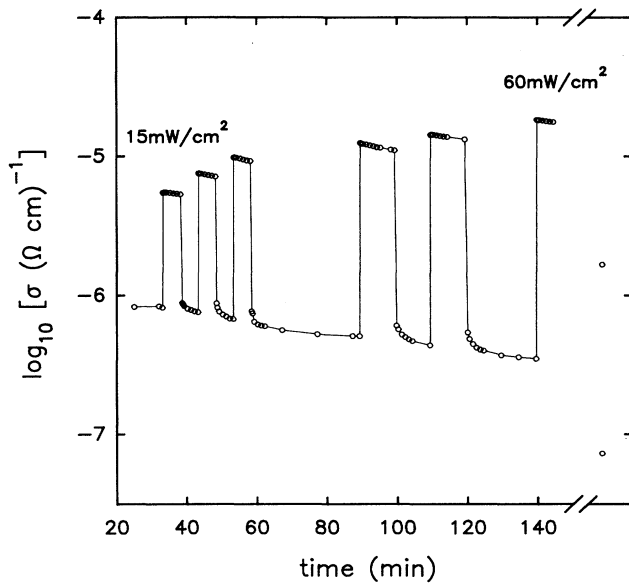


FIG. 3. The illumination of film 1 with increasing white-light intensities from  $\sim 15$  to  $\sim 60$   $\text{mW}/\text{cm}^2$  in a vacuum of  $10^{-7}$  Torr. Notice the decrease in (photo) conductivity during illumination and the lower value of the dark conductivity after illumination. The two data points to the right of the time axis break give the values of the photoconductivity and dark conductivity after a 24-h illumination period with  $60$   $\text{mW}/\text{cm}^2$  white-light intensity.

In order to see if this decrease in  $\sigma$  and  $\sigma_{\text{ph}}$  could be eliminated by annealing at higher temperatures, we proceeded to heat the sample to  $180^\circ\text{C}$  (the deposition temperature). The open triangle data points in Fig. 4 show the  $\sigma$  values measured on heating. A straight-line segment is obtained for the heating curve only above  $165^\circ\text{C}$ . The sample was kept at  $180^\circ\text{C}$  for several hours, but no significant change in  $\sigma$  was observed at this temperature. Finally,  $\sigma$  was measured on cooling, yielding a straight line (open circle data points in Fig. 4) characterized by  $E_a = 0.60$  eV,  $\sigma_0 = 3 \times 10^3$   $(\Omega \text{cm})^{-1}$ . This line is reproduced if one again measures  $\sigma$  on heating or cooling. Thus, after annealing, the sample recovers only partially and is left in a state *B* which is more resistive and has a larger activation energy than the original (before illumination) state *A*, shown as a solid line in Fig. 4 for

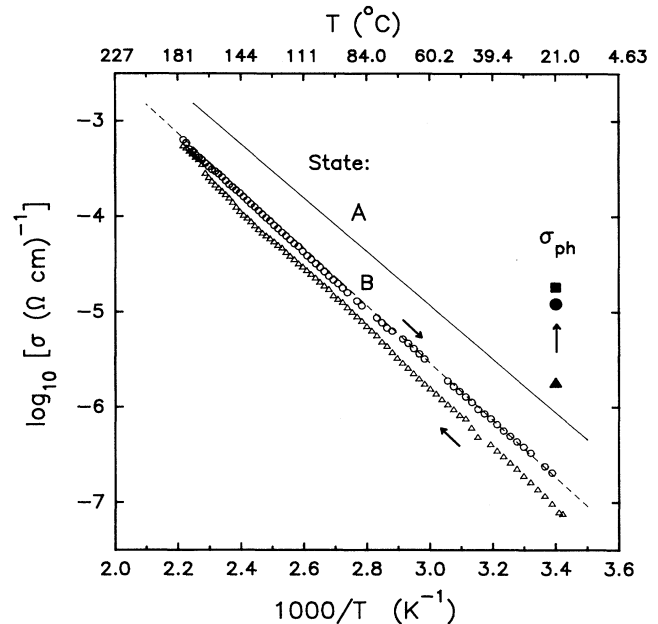


FIG. 4. The conductivity of film 1 measured on heating (triangles) and cooling (circles) after  $\sim 24$ -h illumination with  $60$   $\text{mW}/\text{cm}^2$  white-light intensity in a vacuum of  $10^{-7}$  Torr. The heating and cooling curves meet at  $\sim 165^\circ\text{C}$ . The curve obtained on cooling can be reproducibly traced back and forth as a function of temperature and is thus assigned to a new state *B* of film 1. State *A*, before illumination, is shown as a solid line for comparison. Solid symbols give the room-temperature photoconductivity in the original state *A* (square), after illumination (triangle), and in state *B* (circle).

comparison. It is interesting to note in Fig. 4 that the heating curve smoothly joins the cooling curve at  $T \sim 165^\circ\text{C}$ , indicating that most of the partial recovery of the sample was already completed at this temperature when heating. The solid data points in Fig. 4 give the room-temperature value of  $\sigma_{\text{ph}}$  before (triangle) and after (circle) annealing. The solid square indicates the value of  $\sigma_{\text{ph}}$  in the original state *A*. Table I summarizes the values of  $\sigma$  and  $\sigma_{\text{ph}}$  measured at  $21^\circ\text{C}$ , and  $E_a$  and  $\sigma_0$ , for states *A*, *B*, and states *C*–*E* discussed below. The  $\sigma_{\text{ph}}$  values correspond to a light intensity of  $60$   $\text{mW}/\text{cm}^2$ .

Figure 5 shows the effect of oxygen on  $\sigma$  at  $T = 21^\circ\text{C}$ .

TABLE I. Dark conductivity  $\sigma$  and photoconductivity  $\sigma_{\text{ph}}$  measured at  $21^\circ\text{C}$ , and dark conductivity activation energy  $E_a$  and prefactor  $\sigma_0$  for different states of film 1. The  $\sigma_{\text{ph}}$  values are for a white-light intensity  $F = 60$   $\text{mW}/\text{cm}^2$ . The asterisk indicates a value obtained from Fig. 3 after some film degradation.

State	$\sigma$ $(\Omega \text{cm})^{-1}$	$E_a$ (eV)	$\sigma_0$ $(\Omega \text{cm})^{-1}$	$\sigma_{\text{ph}}$ $(\Omega \text{cm})^{-1}$
<i>A</i>	$8.3 \times 10^{-7}$	0.54	$1.5 \times 10^3$	$*1.9 \times 10^{-5}$
<i>B</i>	$1.8 \times 10^{-7}$	0.60	$3.0 \times 10^3$	$1.2 \times 10^{-5}$
<i>C</i>	$6.4 \times 10^{-8}$	0.63	$4.3 \times 10^3$	
<i>D</i>	$9.8 \times 10^{-9}$	0.68	$5.2 \times 10^3$	$7.5 \times 10^{-6}$
<i>E</i>	$8.3 \times 10^{-12}$	0.79	$3.0 \times 10^3$	$5.5 \times 10^{-9}$
<i>F</i>	$1.5 \times 10^{-14}$	0.95	$2.2 \times 10^2$	

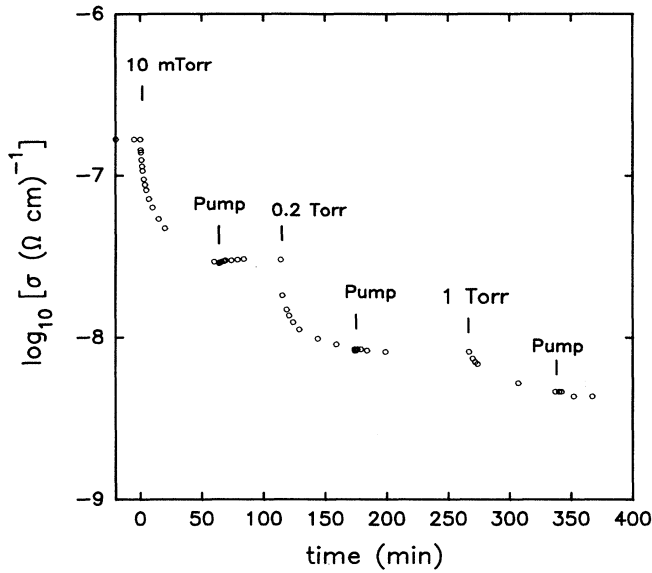


FIG. 5. The effect of pure  $O_2$  on the conductivity of a  $C_{60}$  thin film. At given times, an indicated (dynamic) pressure of  $O_2$  is admitted in the deposition-measurement chamber. At points marked "pump," the oxygen flow is interrupted and the  $10^{-7}$ -Torr vacuum is restored.

Beginning with the sample in state *B*, 10 mTorr of  $O_2$  (dynamic pressure) are admitted in the deposition-measurement chamber. An immediate decrease in  $\sigma$  takes place, and an hour later  $\sigma$  is still decreasing, though at a slower rate. At the point marked "pump" in Fig. 5, corresponding to time = 60 min, the oxygen flow is interrupted and the  $10^{-7}$ -Torr vacuum is restored. No significant recovery in  $\sigma$  occurs over an hour period. We repeat the process with oxygen pressures of 0.2 and 1.0 Torr. At time = 370 min in Fig. 5,  $\sigma$  and  $\sigma_{ph}$  (not shown) have decreased by factors of 40 and 1.6, respectively. Subsequent annealing eliminates most, but not all, of the effect of oxygen on the conductivity, as seen in Fig. 6. The sample was heated (triangles) up to  $180^\circ\text{C}$  and kept at this temperature for several hours, until  $\sigma$  reached a stable value. A reproducible straight line is then obtained upon cooling (and heating), given by the circle data points in Fig. 6. Thus the film is now in a slightly more resistive state *C*, having  $E_a = 0.63$  eV,  $\sigma_0 = 4.3 \times 10^3$   $(\Omega\text{cm})^{-1}$ , and  $\sigma(21^\circ\text{C}) = 6.4 \times 10^{-8}$   $(\Omega\text{cm})^{-1}$ . State *B* is also shown as a solid line in Fig. 6 for comparison. Figure 6 also shows, as did Fig. 4, that most of the partial restoration of the film is already completed at around  $165^\circ\text{C}$  when the heating curve joins the final state *C*.

Figure 7 shows an impressive recovery of more than five orders of magnitude in the value of  $\sigma$  as one heats (triangles) the sample after 12-h exposure in the dark to atmosphere. At the usual rate of  $2^\circ\text{C}/\text{min}$ ,  $\sigma \sim 6 \times 10^{-6}$   $(\Omega\text{cm})^{-1}$  when the temperature  $180^\circ\text{C}$  was reached. At this temperature,  $\sigma$  continued to increase for some 20 h. After a stable (on a time scale of many hours) value of  $\sigma$  was observed at  $180^\circ\text{C}$ ,  $\sigma$  was then measured on cooling, obtaining a reproducible state *D* (circles in Fig. 7) more

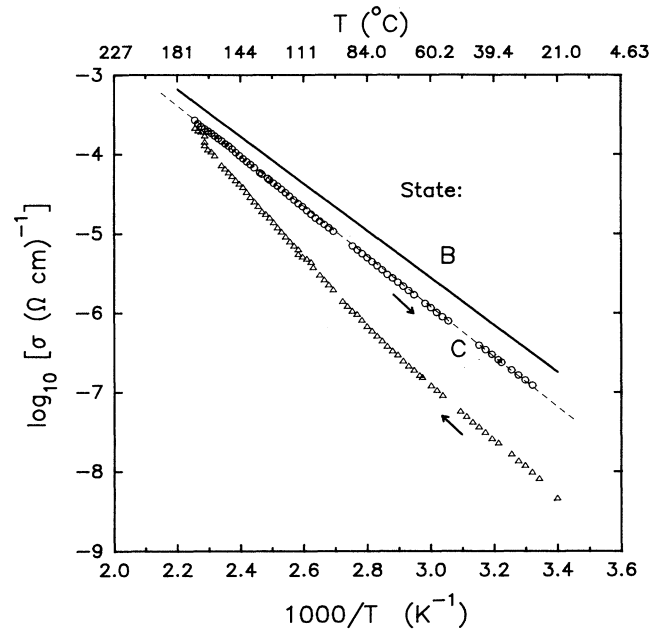


FIG. 6. The behavior of the conductivity of a  $C_{60}$  film after exposure to pure  $O_2$ , as shown in Fig. 5. After heating (triangles) to  $180^\circ\text{C}$ , a reproducible state *C* (circles, dashed line) is obtained. State *B*, before oxygen exposure, is shown as a solid line for comparison.

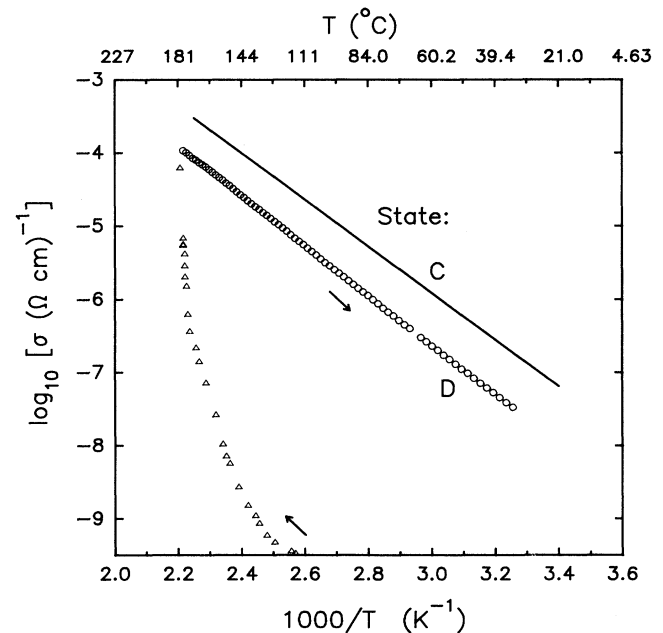


FIG. 7. The annealing behavior of the conductivity of the  $C_{60}$  film after a 24-h exposure to atmosphere (in dark). After heating (triangles) and holding the sample at  $180^\circ\text{C}$  for some 20 h, a reproducible state *D* (circles) is obtained. State *C* (before exposure to atmosphere) is given by the solid line for comparison.

resistive and with a larger activation energy than state *C* (before exposure to atmosphere). State *D* has  $E_a=0.68$  eV,  $\sigma_0=5.2\times 10^3$  ( $\Omega\text{ cm}$ )<sup>-1</sup>, and  $\sigma(21^\circ\text{C})=9.8\times 10^{-9}$  ( $\Omega\text{ cm}$ )<sup>-1</sup>.

In trying to anneal the effects of oxygen exposure on the conductivity of film 1, we did not exceed the sample deposition temperature of 180°C, to avoid possible morphological or structural changes that could have some bearing on the conductivity. In studies on a similar film (film 3) deposited at the same temperature of 180°C, we carried out additional annealings at 230 and 270°C in a vacuum of 10<sup>-7</sup> Torr for a couple of hours each time, resulting in only marginal additional recovery of the conductivity. After further annealing at 290°C for 15 h, the conductivity of film 3 dropped below our detection limit.

We also carried out additional experiments in other C<sub>60</sub> films to verify that nitrogen, argon, and helium gases had no effect on the conductivity. The role of the water vapor in the atmosphere on the observed  $\sigma$  changes, however, remains to be determined. It is well known that water vapor can act as a catalyst to accelerate oxidation in some materials. We also observed that turning on a hot cathode vacuum gauge in the vacuum chamber, thus creating charged gaseous species, had no effect on  $\sigma$  when flowing N<sub>2</sub> or Ar, but accelerated the decrease in  $\sigma$  when flowing O<sub>2</sub>.

We have seen so far that exposing the film to oxygen or atmosphere has the effect of decreasing  $\sigma$  and  $\sigma_{\text{ph}}$ , but most of the effect can be reversed by annealing the sample at temperatures between 160 and 180°C. Illumination in a vacuum of 10<sup>-7</sup> Torr causes a comparatively small decrease in  $\sigma$ , but the effect cannot, for the most part, be reversed by annealing. We show next that the largest irreversible effects are obtained when the sample is simultaneously exposed to light and oxygen.

Starting from state *D*, given by the solid line in Fig. 8, film 1 was illuminated at room temperature for 15 min with 60-mW/cm<sup>2</sup> white-light intensity in 1-atm O<sub>2</sub> (dynamic pressure). The dark conductivity  $\sigma$  decreased several orders of magnitude to a value below our detection limit, and  $\sigma_{\text{ph}}$  (solid square) dropped to a value (solid triangle) a factor  $\sim 10^3$  smaller. The sample was then heated to 180°C (open triangles), and kept at this temperature for several hours until a stable value of  $\sigma$  was observed. The reproducible state *E* (open circles) was then obtained, having  $E_a=0.79$  eV,  $\sigma_0=3\times 10^2$  ( $\Omega\text{ cm}$ )<sup>-1</sup>, and  $\sigma(21^\circ\text{C})=8.3\times 10^{-12}$  ( $\Omega\text{ cm}$ )<sup>-1</sup>. The value of  $\sigma_{\text{ph}}$  in state *E* is given by the solid circle in Fig. 8. State *E* is almost 10<sup>3</sup> times more resistive and has a considerably larger activation energy than state *D*. Finally, Table I shows the values  $\sigma(21^\circ\text{C})=1.5\times 10^{-14}$  ( $\Omega\text{ cm}$ )<sup>-1</sup> and  $E_a=0.95$  eV for state *F*, obtained after 1-h illumination at room temperature in 1 atm O<sub>2</sub> and subsequent annealing at 180°C. The value for  $\sigma(21^\circ\text{C})$  for state *F* was obtained by extrapolation of  $\sigma$  values measured above 80°C.

#### IV. DISCUSSION

There are a number of interesting points to be made about the effect of O<sub>2</sub> on the conductivity of C<sub>60</sub> thin films at room temperature. The immediate decrease in  $\sigma$

observed in Fig. 5 upon admission of 10 m Torr O<sub>2</sub> in the measuring chamber, indicates that O<sub>2</sub> quickly permeates the whole depth of the films. The drop in  $\sigma$  cannot be attributed to a surface effect, because in such a case the still more conductive bulk would short the surface and no decrease in  $\sigma$  would be observed. The decrease of  $\sigma$ , however, does not saturate quickly and continues for hours at a given O<sub>2</sub> pressure, suggesting some kind of activated process for the intake of oxygen. The annealing behavior observed in Figs. 6 and 7 indicates that most of the absorbed oxygen can be expelled out of the film by increasing the temperature to 160–180°C in vacuum. A comparatively small degradation persists after annealing. We attribute this degradation to a small amount of remnant oxygen or to the destruction of a small percentage of the C<sub>60</sub> molecules in the film, in a way similar to that observed at an accelerated rate in pure O<sub>2</sub> at temperatures of 200°C.<sup>23</sup>

The reversible conductivity effects of O<sub>2</sub> absorption can be explained qualitatively as follows. Oxygen penetrates the whole depth of a C<sub>60</sub> film at a rate that depends on the applied partial pressure of oxygen gas. One or more oxygen atoms physically attach to the surface of C<sub>60</sub> molecules. This physisorption is strong enough to prevent the escape of the oxygen from the film upon restoring high vacuum in the measuring chamber, but weak enough to allow the release of most of the oxygen at moderate tem-

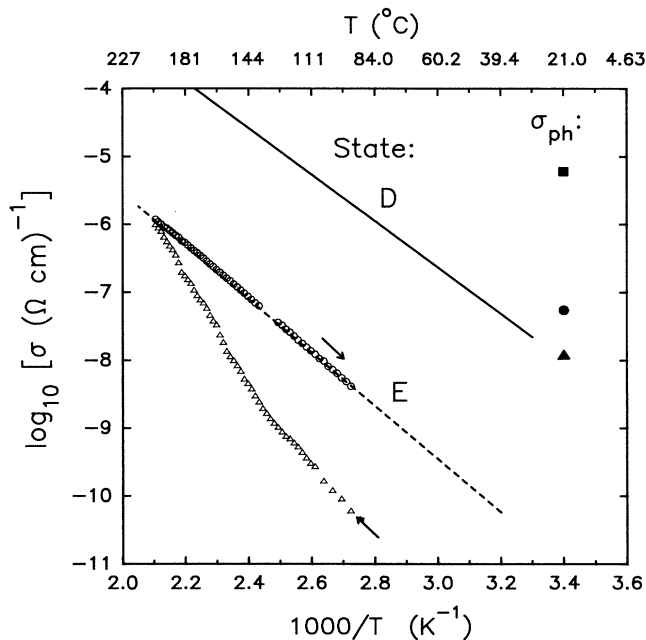


FIG. 8. The effect on  $\sigma$  of 15-min illumination with 60-mW/cm<sup>2</sup> white-light intensity in 1-atm O<sub>2</sub>. After illumination, the sample is heated (triangles) to 180°C, and a reproducible state *E* is obtained, being much more resistive and having a considerably higher activation energy than the original state *D* (see also Table I). The solid symbols show the room-temperature photoconductivity  $\sigma_{\text{ph}}$  in state *D* (square), after illumination (triangle), and in state *E* (circle).

peratures of about 170 °C. The oxygen within the bulk of solid C<sub>60</sub> generates a disorder potential that localizes and shifts, toward the gap, electronic states at the band edges of the semiconductor. In addition, oxygen may act as an efficient trap for electrons in the conduction band of C<sub>60</sub>. The new defect and impurity gap states can then act as trapping and recombination centers that decrease the carriers lifetime and drift mobilities in the semiconductor. These changes in electronic-state density would lead to an increase in the measured activation energy and a decrease in the dark conductivity and photoconductivity. Reference 32 calculated the way in which attachment of oxygen atoms to the surface of the C<sub>60</sub> molecule leads to the localization and energy shifting of electronic states in the highest-occupied-molecular-orbital (HOMO) and lowest-unoccupied-molecular-orbital (LUMO) bands of the C<sub>60</sub> molecule. There, however, it was assumed that an oxygen atom bonds to two adjacent carbon sites whose previous common bond is destroyed. It is unlikely that such C-O bonds would form spontaneously at room temperature in the absence of light, and those would dissociate at temperatures of 160 °C.

Illumination of a sample in an O<sub>2</sub> atmosphere seems to provide the required energy to stimulate the irreversible reactions leading to formation of C-O compounds.<sup>23–25</sup> The resulting disorder potential and the large number of broken molecules left behind must remove and localized many of the states at the band edges, increasing the resistivity and activation energy of the film, as shown by state *E* in Fig. 8. The partial recovery of the sample upon annealing, as seen in Fig. 8, may be due to the expulsion of nonreacted oxygen (reversibly attached to the C<sub>60</sub> molecule) and some of the C-O compound molecules. The relatively small conductivity changes produced by light in a vacuum of 10<sup>-7</sup> Torr (Fig. 6) are perhaps due to the small amount of oxygen present. This is supported by experiments showing that illumination of C<sub>60</sub> films at 20 K in a vacuum ~10<sup>-10</sup> Torr produces no changes in photoemission spectra.<sup>25</sup>

It is interesting to mention here that highly sensitive photothermal deflection spectroscopy measurements of the optical-absorption spectrum of C<sub>60</sub> thin films have been carried out in the range 0.4–2.5 eV.<sup>33</sup> These measurements reveal a gap region that includes an Urbach edge from 1.5 to 1.8 eV, and a weaker subgap absorption shoulder between 0.8 and 1.5 eV. The Urbach edge, a region where the absorption coefficient varies exponentially with photon energy, is associated in amorphous semiconductor physics with an exponentially decaying density of localized electronic states extending from the band edge into the gap, and is believed to be caused by disorder. The possibility of the subgap absorption in C<sub>60</sub> being caused by a carbon dangling bond (unpaired electron orbital) has been noted,<sup>35</sup> a possibility that is consistent with observations of an electron-spin-resonance (ESR) signal from the C<sub>60</sub> films.<sup>33</sup> Good-quality C<sub>60</sub> powder samples appear to have no ESR signal, but a resonance develops after brief exposure of the powder to air or oxygen at room temperature. Subsequent evacuation of the sample vessel, however, largely eliminates the resonance. Exposure of the powder samples to air or oxygen at

higher temperatures results in the appearance of a permanent ESR signal.<sup>34</sup>

The origin of the downward curvature on the  $\sigma$  versus  $1/T$  curve [Fig. 2(b)] observed in thicker C<sub>60</sub> films (>200 nm) is not clear at this time. Perhaps it is the result of a large and temperature-dependent volume expansion coefficient for this Van der Waals solid, for which the primary effect of a lattice expansion on the electronic structure is the narrowing of the electronic bands and the widening of the energy gaps. The absence of a curvature in the  $\sigma$  versus  $1/T$  curve in thin (<200-nm) films could be understood if the first few layers near the C<sub>60</sub>/substrate interface are restricted to expand and contract with the more rigid sapphire substrate.

The *in situ* activation energies of 0.54–0.57 eV imply an electronic (transport) band gap for C<sub>60</sub> of about 1.1 eV, assuming a Fermi level near midgap. Microscopic total-energy calculations<sup>35</sup> and OLCAO (orthogonalized linear combination of atomic orbitals) calculations<sup>36</sup> in the local-density approximation predict C<sub>60</sub> to be a semiconductor with an optically forbidden direct energy gap at the *X* point of the Brillouin zone. Reported calculated values for the fundamental gap include 1.5,<sup>37</sup> 1.34,<sup>36</sup> and 0.98 eV.<sup>8</sup> The first optically allowed transition is expected at about 1.8 eV.<sup>36</sup> Optical and electron-scattering measurements have yielded gap values in the range 1.5–2.3 eV.<sup>9,33,37–40</sup> In conductivity measurements, thermalization processes of electrons and holes populate the top and bottom of the valence and conduction bands, respectively, and the direct gap can be obtained from the intrinsic activation energy. It is important to note, however, that the extreme sensitivity of the Fermi-level position to the presence of doping impurities in some semiconductors may make it very difficult to obtain the activation energy of the intrinsic material. Presently, we do not know whether C<sub>60</sub> powder, synthesized and processed according to standard techniques, may contain active dopant impurities in concentrations of a few parts per million or less, and whether these active impurities would be present in the film.

## V. SUMMARY AND CONCLUSIONS

*In situ* dc conductivity measurements in the range 20–180 °C of C<sub>60</sub> polycrystalline films deposited at 180 °C reveal clear semiconductor behavior. At room temperature, O<sub>2</sub> gas quickly diffuses into the bulk of our C<sub>60</sub> films and changes the electronic transport properties of the material, and in particular decreases the conductivity and photoconductivity by orders of magnitude. These changes may originate when oxygen physically attaches to the C<sub>60</sub> molecule, generating a disorder potential that localizes electronic states in the top of the HOMO- and the bottom of the LUMO-derived bands of the solid. In addition, oxygen may act as an efficient trap for electrons in the conduction band of C<sub>60</sub>. The effects of oxygen can be mostly reversed by increasing the sample temperature above 170 °C in vacuum, probably due to the expulsion of oxygen from the C<sub>60</sub> film. Exposure of C<sub>60</sub> films to N<sub>2</sub>, Ar, and He gases had no effect on the film conductivities. Light should not alter films containing no oxygen and in

ultrahigh vacuum. The combination of light and oxygen induces a large irreversible decrease in the conductivity and photoconductivity of  $C_{60}$  films, probably due to the light-promoted formation of carbon-oxygen compounds that leaves behind a large number of broken  $C_{60}$  molecules. Measured optical properties of  $C_{60}$ , especially in the low-photon-energy range, may be affected by oxygen contamination and strong light.

#### ACKNOWLEDGMENTS

The authors would like to thank Dr. C. W. Chu for his advice and support. This work was funded in part by the NSF Grant No. DMR 86-126539 (CWC), DARPA Grant No. MDA 972-88-G-002, NASA Grant No. NAGW-977, Texas Center for Superconductivity at the University of Houston, and the T. L. L. Temple Foundation.

- <sup>1</sup>H. W. Kroto, J. R. Heath, S. C. O'Brian, R. F. Curl, and R. E. Smalley, *Nature* **318**, 162 (1985).
- <sup>2</sup>W. Kratschmer, L. D. Lamb, K. Fostiropoulos, and D. R. Huffman, *Nature* **347**, 354 (1990).
- <sup>3</sup>A. F. Hebard, M. J. Rosseinsky, R. C. Haddon, D. W. Murphy, S. H. Glarum, T. T. M. Palstra, A. P. Ramirez, and A. R. Kortan, *Nature* **350**, 600 (1991).
- <sup>4</sup>M. J. Rosseinsky, A. P. Ramirez, S. H. Glarum, D. W. Murphy, R. C. Haddon, A. F. Hebard, T. T. M. Palstra, A. R. Kortan, S. M. Zahurak, and A. V. Makhija, *Phys. Rev. Lett.* **66**, 2830 (1991).
- <sup>5</sup>S. P. Kelty, C. C. Chen, and C. M. Lieber, *Nature* **352**, 223 (1991).
- <sup>6</sup>K. Tanigaki, T. W. Ebbesen, S. Saito, J. Mizuki, J. S. Tsai, Y. Kubo, and S. Kuroshima, *Nature* **352**, 222 (1991).
- <sup>7</sup>J. Mort, K. Okumura, M. Machonkin, R. Ziolo, D. R. Huffman, and M. I. Ferguson, *Chem. Phys. Lett.* **186**, 281 (1991).
- <sup>8</sup>J. Mort, R. Ziolo, M. Machonkin, D. R. Huffman, and M. I. Ferguson, *Chem. Phys. Lett.* **186**, 284 (1991).
- <sup>9</sup>J. Mort, M. Machonkin, R. Ziolo, D. R. Huffman, and M. I. Ferguson, *Appl. Phys. Lett.* **60**, 1735 (1992).
- <sup>10</sup>P. J. Benning, J. L. Martins, J. H. Weaver, L. P. F. Chibante, and R. E. Smalley, *Science* **252**, 1417 (1991).
- <sup>11</sup>J. H. Weaver, J. L. Martins, T. Komeda, Y. Chen, T. R. Ohno, G. H. Kroll, N. Troullier, R. E. Hauffer, and R. E. Smalley, *Phys. Rev. Lett.* **66**, 1741 (1991).
- <sup>12</sup>R. M. Flemming, T. Siegrist, P. M. Marsh, B. Hessen, A. R. Kortan, D. W. Murphy, R. C. Haddon, R. Tycko, G. Dabbagh, A. M. Muzsca, M. L. Kaplan, and S. M. Zahurak, in *Clusters and Cluster-Assembled Materials*, edited by R. S. Averback, J. Bernhole, and O. L. Nelson, MRS Symposia Proceedings No. 206 (Materials Research Society, Pittsburgh, 1990), p. 691.
- <sup>13</sup>R. C. Haddon, L. E. Brus, and K. Raghavachari, *Chem. Phys. Lett.* **131**, 165 (1986).
- <sup>14</sup>P. A. Heiney, J. E. Fisher, A. R. McGhie, W. J. Romanow, A. M. Denenstein, J. P. McCauley, Jr., A. B. Smith, and D. E. Cox, *Phys. Rev. Lett.* **66**, 2911 (1991).
- <sup>15</sup>D. Dubois, K. M. Kadish, S. Flanigan, R. E. Hauffer, L. P. F. Chibante, and L. J. Wilson, *J. Am. Chem. Soc.* **113**, 4364 (1991).
- <sup>16</sup>Y. Chai, T. Guo, C. Jin, R. E. Hauffer, L. P. F. Chibante, J. Fure, L. Wang, J. M. Alford, and R. E. Smalley, *J. Phys. Chem.* **95**, 7564 (1991).
- <sup>17</sup>J. Cioslowski and E. D. Fleischman, *J. Chem. Phys.* **94**, 3730 (1991).
- <sup>18</sup>A. H. H. Chang, W. C. Ermler, and R. M. Pitzer, *J. Chem. Phys.* **94**, 5004 (1991).
- <sup>19</sup>S. Saito (unpublished).
- <sup>20</sup>A. F. Hebard, in *Physics and Chemistry of Finite Systems: From Clusters to Crystals*, edited by P. Jena, S. N. Khanna, and B. K. Rao (Kluwer, Dordrecht, 1992).
- <sup>21</sup>S. J. Duclos, R. C. Haddon, S. H. Glarum, A. F. Hebard, and K. B. Lyons, *Solid State Commun.* **80**, 481 (1991).
- <sup>22</sup>K. Matsuishi, R. L. Meng, Y. T. Ren, P. H. Hor, and C. W. Chu, in *Proceedings of the TCSUH Workshop on High Temperature Superconducting Materials, Bulk Processing, and Bulk Applications, 1992, Houston, Texas*, edited by C. W. Chu, W. K. Chu, P. H. Hor, and K. Salama (World Scientific, Singapore, 1992), p. 205.
- <sup>23</sup>H. S. Chen, A. R. Kortan, R. C. Haddon, M. K. Kaplan, C. H. Chen, A. M. Muzsca, H. Chou, and D. A. Fleming, *Appl. Phys. Lett.* **59**, 2956 (1991).
- <sup>24</sup>A. M. Vasallo, L. S. K. Pang, P. A. Cole-Clarke, and M. A. Wilson, *J. Am. Chem. Soc.* **113**, 7820 (1991).
- <sup>25</sup>G. H. Kroll, P. J. Benning, Y. Chen, T. R. Ohno, J. H. Weaver, L. P. F. Chibante, and R. E. Smalley, *Chem. Phys. Lett.* **181**, 112 (1991).
- <sup>26</sup>R. Taylor, J. P. Parsons, A. G. Avent, S. P. Rannard, T. J. Dennis, J. P. Hare, H. W. Kroto, and D. R. M. Walton, *Nature* **351**, 277 (1991).
- <sup>27</sup>R. C. Haddon, A. F. Hebard, M. J. Rosseinsky, D. W. Murphy, S. J. Duclos, K. B. Lyons, B. Miller, J. M. Rosamilia, R. M. Fleming, A. R. Kortan, S. H. Glarum, A. V. Makhija, A. J. Muller, R. H. Eick, S. M. Zahurak, R. Tycko, G. Dabbagh, and F. A. Thiel, *Nature* **350**, 320 (1991).
- <sup>28</sup>G. P. Kochanski, A. F. Hebard, R. C. Haddon, and A. T. Fiory, *Science* **255**, 184 (1992).
- <sup>29</sup>W. Kratschmer, L. D. Lamb, K. Fostiropoulos, and D. R. Huffman, *Nature* **347**, 354 (1990).
- <sup>30</sup>H. Aije, M. M. Alvarez, S. J. Anz, R. D. Beck, F. Diederich, K. Fostiropoulos, D. R. Huffman, W. Kratschmer, Y. Rubin, K. E. Schriver, D. Sensharma, and R. L. Whetten, *J. Phys. Chem.* **94**, 8630 (1990).
- <sup>31</sup>Y. Z. Li, M. Chander, J. C. Patrin, J. H. Weaver, L. P. F. Chibante, and R. E. Smalley, *Science* **253**, 429 (1991).
- <sup>32</sup>K. Harigaya, *J. Phys.* **4**, 6769 (1992).
- <sup>33</sup>A. Skumanich, *Chem. Phys. Lett.* **182**, 486 (1991).
- <sup>34</sup>L. Kevan (private communication).
- <sup>35</sup>S. Saito and A. Oshiyama, *Phys. Rev. Lett.* **66**, 2637 (1991).
- <sup>36</sup>W. Y. Ching, M. Z. Huang, Y. N. Xu, W. G. Harter, and F. T. Chan, *Phys. Rev. Lett.* **67**, 2045 (1991).
- <sup>37</sup>P. L. Hansen, P. J. Fallon, and W. Kratschmer, *Chem. Phys. Lett.* **181**, 367 (1991).
- <sup>38</sup>A. Lucas, G. Gensterblum, J. J. Pireaux, P. A. Thiry, R. Caudano, J. P. Vigneron, P. Lambin, and W. Kratschmer, *Phys. Rev. B* **45**, 3694 (1992).
- <sup>39</sup>M. K. Kelly, P. Etchegoin, D. Fuchs, W. Kratschmer, and K. Fostiropoulos, *Phys. Rev. B* **46**, 4963 (1992).
- <sup>40</sup>S. L. Ren, Y. Wang, A. M. Rao, E. McRae, J. M. Holden, T. Hager, K. Wang, W. T. Lee, H. F. Ni, J. Selegue, and P. C. Eklund, *Appl. Phys. Lett.* **69**, 2678 (1991).